Retrograde BMP Signaling Regulates Trigeminal Sensory Neuron Identities and the Formation of Precise Face Maps

Liberty K. Hodge,[1,2] Matthew P. Klassen,[3] Bao-Xia Han,[1] Glenn Yiu,[4] Joanna Hurrell,[4] Audrey Howell,[2]
Guy Rousseau,[5] Frederic Lemaigre,[5] Marc Tessier-Lavigne,[6] and Fan Wang[1,2,*]
[1] Department of Cell Biology
[2] Developmental Biology Training Program
Duke University Medical Center, Box 3709, Durham, NC 27710, USA
[3] Department of Biological Sciences, Stanford University, Stanford CA 94305, USA
[4] Department of Neurology, Children's Hospital, Harvard University, Boston, MA 02115, USA
[5] Universite Catholique de Louvain, Institute of Cellular Pathology, Avenue Hippocrate 75, 7529, 1200 Brussels, Belgium
[6] Genentech Inc., One DNA Way, South San Francisco, CA 94080, USA
*Correspondence: f.wang@cellbio.duke.edu
DOI 10.1016/j.neuron.2007.07.010

SUMMARY

Somatosensory information from the face is transmitted to the brain by trigeminal sensory neurons. It was previously unknown whether neurons innervating distinct areas of the face possess molecular differences. We have identified a set of genes differentially expressed along the dorsoventral axis of the embryonic mouse trigeminal ganglion and thus can be considered trigeminal positional identity markers. Interestingly, establishing some of the spatial patterns requires signals from the developing face. We identified bone morphogenetic protein 4 (BMP4) as one of these target-derived factors and showed that spatially defined retrograde BMP signaling controls the differential gene expressions in trigeminal neurons through both Smad4-independent and Smad4-dependent pathways. Mice lacking one of the BMP4-regulated transcription factors, *Onecut2 (OC2),* have defects in the trigeminal central projections representing the whiskers. Our results provide molecular evidence for both spatial patterning and retrograde regulation of gene expression in sensory neurons during the development of the somatosensory map.

INTRODUCTION

In all vertebrate species, somatic stimuli from the face are transmitted to the somatosensory centers in the central nervous system (CNS) by the conserved trigeminal sensory neurons. In rodent, from the trigeminal ganglion, three distinct peripheral axon bundles are formed to innervate three primary regions of the face: ophthalmic, maxillary, and mandibular areas (Figure 1A and also Waite and Tracey, 1995). Newly born trigeminal neurons immediately choose one of the three pathways to extend a peripheral axon while simultaneously projecting a central axon into the brainstem (O'Connor and Tessier-Lavigne, 1999). Later, the central axons sprout out interstitial axonal collaterals that project into several brainstem nuclei, generating a set of inverted somatotopic maps representing the face inside the brain (Figure 1E and also Waite and Tracey, 1995). Within the maxillary region of the ganglion, a population of neurons sends peripheral axons to innervate the whiskers on the face. Their central axons in turn form modular synapses known as "barrelette" structures that represent individual whiskers. Notably, the pattern and number of whiskers on the face are precisely replicated by barrelettes in the brainstem, with a one-barrelette-one-whisker relationship (Figure 1E, also reviewed by Killackey et al., 1995). However, the molecular mechanisms employed by trigeminal neurons to transform the spatial information of the face into spatial maps within the brain are largely unknown.

Previous studies of somatic sensory neurons resided in the dorsal root ganglia (DRG) have revealed that there are specific transcription programs regulating distinct aspects of neuronal development and differentiation, including the early specification of sensory lineage (Anderson, 1999; Knecht and Bronner-Fraser, 2002), axon outgrowth (Graef et al., 2003), axon pathfinding (Arber et al., 2000; Inoue et al., 2002), as well as differentiation into specific sensory modalities (Chen et al., 2006a, 2006b; Kramer et al., 2006; Marmigere et al., 2006; Yoshikawa et al., 2007). However, whether there are also transcription factors that specify the positional identities of DRG neurons with regard to their body targets is currently unknown. Another interesting aspect of somatosensory neuron development is the influence of target-derived signals on their differentiation and maturation. For
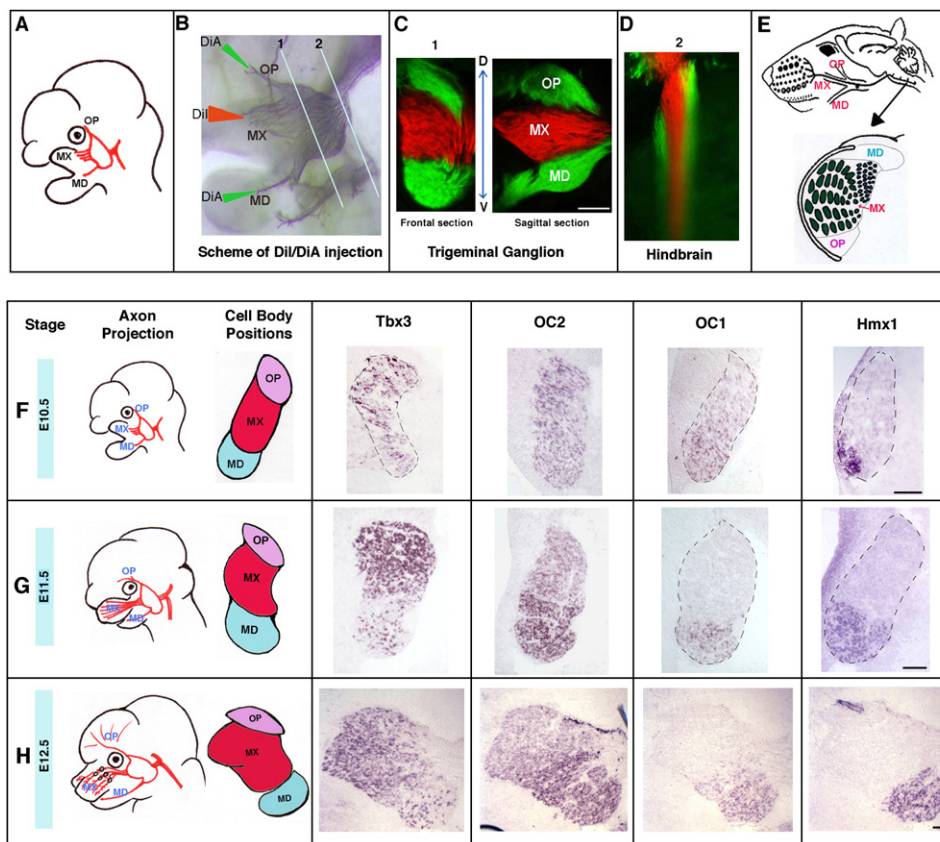
Figure 1. Somatotopic Segregation and Positional Patterning of the Three Trigeminal Divisions

(A) Schematic drawing of E10.5 mouse head showing the location of the trigeminal ganglion, the initial outgrowth of trigeminal axons, and the developing craniofacial structures.

(B) DiA and DiI crystals are placed in the peripheral trigeminal nerves in fixed E10.5 embryos to retrogradely label cell bodies and central axons.

(C) Frontal and sagittal sections of dye-labeled trigeminal ganglion show spatial segregation of the three divisions: ophthalmic neurons in the dorsal part of the ganglion, maxillary neurons in the middle, and mandibular neurons in the ventral domain.

(D) A frontal section shows ordered projections of central trigeminal axons alongside the hindbrain.

(E) Schematic drawing of the adult mouse head, trigeminal ganglion, and trigeminal central nucleus *Interpolaris*, showing the pattern of barrelettes representing the whiskers.

(F–H) In situ hybridization reveals spatial patterns of genes encoding four transcription factors (*Tbx3*, *OC2*, *OC1*, and *Hmx1*) within the E10.5 (F), E11.5 (G), and E12.5 (H) trigeminal ganglion.

*OP, MX, and MD = ophthalmic, maxillary, and mandibular neurons/axons, respectively. 1 and 2 illustrate the plane of the two sections in (C) and (D). Scale bar is 100 μm.

example, periphery-derived neurotrophins are not only essential for the survival of DRG neurons (Ginty and Segal, 2002), but also for their axonal innervation of the skin (Patel et al., 2000); target-derived NT3 is necessary for inducing the ETS transcription factor Er81 expression in proprioceptive neurons (Hippenmeyer et al., 2004; Patel et al., 2003); Activin expressed in skin tissue induce the expression of neuropeptide CGRP in DRG neurons (Ai et al., 1999; Hall et al., 2001; Xu et al., 2005), and artificial manipulation of the amount of skin-derived BMPs can alter the number of trigeminal sensory neurons and the extent of their peripheral innervation (Guha et al., 2004). Thus, retrograde signaling from targets to cell bodies plays important roles in sensory neuron development.

But whether peripheral targets can also retrogradely specify the positional identities of sensory neurons is unknown.

To begin to understand the question of spatial patterning in the trigeminal ganglia, we first performed microarray gene expression analyses on neurons projecting to the three distinct areas of the face. We identified a set of genes that are differentially expressed along the dorsoventral axis of the trigeminal ganglion and thus can roughly be considered as positional identity markers. Using these tools, we obtained evidence for target-derived influences on the positional patterning of these neurons and identified some of the molecular components of this retrograde specification mechanism.

RESULTS

Early Somatotopic Organization of Trigeminal Ganglia and the Identification of Positional Differences among Trigeminal Neurons

In initial experiments, we placed two lipophilic dyes (DiI and DiA) individually into each of the developing target regions of the three trigeminal nerves in fixed E10.5 mouse embryos (Figure 1B). This permitted the retrograde labeling of neuronal cell bodies within the ganglion. We found that trigeminal neurons projecting into the three peripheral branches are spatially segregated into three distinct groups along the dorsoventral axis of the ganglion: (1) a relatively small, dorsal-most domain of ophthalmic projecting neurons; (2) a large middle region corresponding to neurons projecting into the maxillary arch; and (3) a ventral division of mandibular-innervating neurons (Figure 1C). Moreover, the main central axons are also organized into three ordered parallel tracks (Figure 1D). Thus, there is an early somatotopic organization of both the neuronal bodies and the major axonal tracks in the trigeminal system. This finding is consistent with previous studies in various species (Beaudreau and Jerge, 1968; Borsook et al., 2003; Erzurumlu and Jhaveri, 1992; Scott and Atkinson, 1999). The segregation allowed us to obtain neurons projecting to distinct facial areas (ophthalmic, maxillary, and mandibular neurons) by microdissecting 500 E11.5 trigeminal ganglia (TG) and comparing gene expression patterns among them by genome-wide analysis. In this way, we identified a set of molecular markers that exhibit distinct spatial patterns of expression within the E11.5 TG. We focused on four transcription factors for further analyses as described below. (Details of the microarray studies and the list of genes confirmed by in situ hybridization experiments can be found in Supplemental Experimental Procedures and Table S1 in the Supplemental Data available with this article online).

A Set of Transcription Factors Can Be Considered Positional Markers for TG Sensory Neurons

At E11.5 (Figure 1G), the gene encoding Tbx3, a T box family transcription factor (Coll et al., 2002), is expressed in all ophthalmic TG neurons, as well as in approximately the dorsal half of the maxillary TG, and a few scattered mandibular neurons. The gene encoding Onecut2 (OC2), a cut-domain-containing homeobox transcription factor (Jacquemin et al., 1999, 2003b) shows differential levels of expression along the dorsoventral axis: it is expressed strongly in the ventral half of the maxillary TG and in the majority of the mandibular neurons, but weakly in the ophthalmic and the dorsal half of the maxillary regions. The expression of Onecut1 (OC1, also called HNF6), a gene encoding another cut homeobox protein (Clotman et al., 2002; Jacquemin et al., 2003a), is primarily limited to mandibular neurons and is also transcribed in a narrow, most ventral stripe of the maxillary TG at this age. Finally, Hmx1, a homeobox factor (Adamska et al., 2001) shows specific expression in mandibular region.

We next addressed when TG neurons acquire these position-dependent differences in gene expression. At E10.5 when the TG axon outgrowth has just initiated (Figure 1F), the spatial patterns are not identical to those seen at E11.5. Strong Tbx3 is seen in fewer scattered cells, with a low-level expression throughout the TG. OC2 is uniformly expressed in the ganglia at this stage. The expression of OC1 is less restricted compared to that typically observed at E11.5. It extends into the dorsal part of the ganglion. Only Hmx1 shows the same mandibular restricted pattern as in the E11.5 embryo. Thus, it appears that the expression patterns of Tbx3, OC2, and OC1 change as the trigeminal axons grow into their peripheral targets from E10.5 to E11.5. We also examined TG at E12.5 and E16.5 and found that the expression patterns of the four transcription factors are largely similar to those at E11.5, with the level of OC2 further reduced in the dorsal region of the TG (Figure 1H for E12.5 and data not shown for E16.5).

Position-Dependent Pattern of Gene Expression Is Not an Intrinsic Property of Trigeminal Ganglion Neurons

Having observed positional differences between trigeminal sensory neurons in vivo, we asked whether these identities are intrinsic and cell autonomously sustained in these neurons or whether their acquisition or maintenance requires extrinsic signals. To assess this, we cultured trigeminal ganglia isolated from E11.5 embryos in vitro for 16–24 hr either in media alone or in media supplemented with neurotrophins (NTs). In media alone, these transcription factors are either not expressed (Tbx3 and Hmx1) or weakly expressed (OC2 and OC1) in trigeminal neurons (Table 1, first column, and data not shown). This is not a result of cell death because TG isolated from $Bax^{-/-}$ embryos, in which neuronal apoptosis is prevented, gave essentially the same results (data not shown). Furthermore, we performed anti-NeuN staining (which detects all postmitotic neurons) together with TUNEL staining (which reveals apoptotic cells), and found that although there is cell death, only less than 1% of the TUNEL positive cells are also NeuN positive (Figure S1). This indicates that all the live neurons under this culture condition do not express appreciable levels of the transcription factors. Thus, the positional differences in gene expression observed in vivo are not stable intrinsic properties of trigeminal neurons since they cannot be maintained in culture.

Next, we cultured TG in media supplemented with neurotrophins. Both NGF and NT3 were added since these two factors were shown to support the survival and growth of the majority of trigeminal neurons at this stage (Huang et al., 1999a; O'Connor and Tessier-Lavigne, 1999). Again, less than 1% of NeuN-positive cells are also TUNEL positive (Figure S1). Interestingly, in the presence of NTs, most of the NeuN staining appears around the outer edge of the ganglion leaving the center barely stained. Perhaps axon outgrowth induced by the NTs caused the migration

Table 1. Quantification of Trigeminal Ganglia Culture Experiments

		Medium Alone	With BMP4	With NTs	With NTs Plus BMP4
% of NeuN-positive cells expressing the marker	Tbx3	ND	39.6% ± 1.5%	ND	89.2% ± 1.5%
	OC2	ND	ND	92.4% ± 2.0%	96.4% ± 0.7%
	OC1	ND	ND	95.6% ± 2.0%	71.1% ± 4.5%
	Hmx1	ND	ND	18.7% ± 1.2%	21.3% ± 1.2%[b]
Spatial distribution index (I_d/I_v ratio)	Tbx3	ND	1.05 ± 0.20	ND	1.24 ± 0.09 (p = 0.11)
	OC2	ND	ND	1.13 ± 0.28	0.76 ± 0.09 (p = 0.18)
	OC1	ND	ND	0.93 ± 0.08	0.48 ± 0.05**
	Hmx1	ND	ND	1.26 ± 0.54	0.25 ± 0.03**
Relative highest signal Intensity	Tbx3	1.0% ± 5.7%	81.8% ± 3.1%	10.1% ± 3.7%	100% ± 1.3%**
	OC2	21.4% ± 4.1%	26.6% ± 7.0%	100% ± 2.9%	47.6% ± 4.5%**
	OC1[a]	43.9% ± 3.0%	34.6% ± 2.3%	100% ± 3.2%	76.4% ± 3.9%**
	Hmx1[a]	6.0% ± 7.9%	1.0% ± 7.9%	100% ± 10.8%	88.4% ± 8.1%

**p < 0.01. The comparison was done between the "with NTs plus BMP4" results and the "with NTs" results for OC2, OC1, and Hmx1; or between the "with NTs plus BMP4" results and the "with BMP4" results for Tbx3. Details of quantification can be found in Supplemental Experimental Procedures.
[a] The highest signal intensity for OC1 and for Hmx1 is in the mandibular region.
[b] Only the cells strongly express Hmx1 are counted.

of the cell bodies to the edge. All quantifications of in situ results involve only NeuN-stained cells. An example for Tbx3 in situ hybridizaton and NeuN immunofluorescence on the same section is shown in Figure S2.

In the presence of NTs, the expression of *Tbx3* was still barely detectable, *OC2* and *OC1* were expressed at relatively high levels in more than 90% of neurons throughout the ganglion, and *Hmx1* was detected in a small subset (20%) of trigeminal neurons scattered across the ganglion without any discernable spatial pattern (Figure 2A and Table 1, third column). These findings indicate that NTs are not sufficient to maintain *Tbx3* expression but are necessary and sufficient to induce/maintain *OC1* and *OC2* expression. As to *Hmx1* transcription, NTs are necessary but not sufficient for maintaining the spatially restricted expression pattern (also see below). Similar results were obtained for cultured E10.5 trigeminal ganglia (data not shown).

To carefully examine whether there are any spatial differences in the expression of *OC2*, *OC1*, and *Hmx1* induced by NTs, we compared the average in situ signal intensity (per unit area) in the dorsal one-third of the trigeminal ganglion (I_d) to that in the ventral one-third of ganglion (I_v) and expressed the results as a ratio of I_d/I_v (illustrated in Figure 2D). Ratios that deviate significantly from 1.0 are indicative of differential expression. No statistically significant differences were detected between dorsal and ventral trigeminal ganglion for these three genes in NT-treated cultures (Figure 2D and Table 1, third column). Thus, uniform application of NTs to TG neither maintains

nor generates spatial differences of transcription factor expression among the TG divisions. Since the neurotrophins are equally expressed along the pathways and in target areas of the three trigeminal nerves during development (O'Connor and Tessier-Lavigne, 1999), it appears that extrinsic signals other than neurotrophins must be present in vivo for the induction or maintenance of *Tbx3* expression, as well as for the suppression of neurotrophin-induced *OC1*, *OC2*, and *Hmx1* in dorsal (ophthalmic and maxillary) TG neurons.

BMP4 Regulates the Expression of Positional Identity Genes in Trigeminal Neurons In Vitro

In order to identify the "extrinsic factor(s)," we first cultured E10.5 trigeminal ganglia together with the eye, and the maxillary and mandibular arches, such that the peripheral axons of the trigeminal neurons were left intact in the developing facial tissues. We found that positional differences in the expression of the four transcription factors can be partially restored/maintained in such cocultures (Figure S3 and data not shown). This implies that the extrinsic signal(s) comes from the developing craniofacial targets. We took a candidate approach and tested whether sonic hedgehog (SHH), FGF8, retinoic acid, WNTs (by using GSK3 inhibitors), or BMP4 can affect the expression of the transcription factors. Only BMP4 had major effects (data not shown for negative results of other factors). In the TG cultures supplemented with both NTs and 20 ng/ml BMP4, we observed a dramatic increase in *Tbx3* expression (Figure 2C), a significant
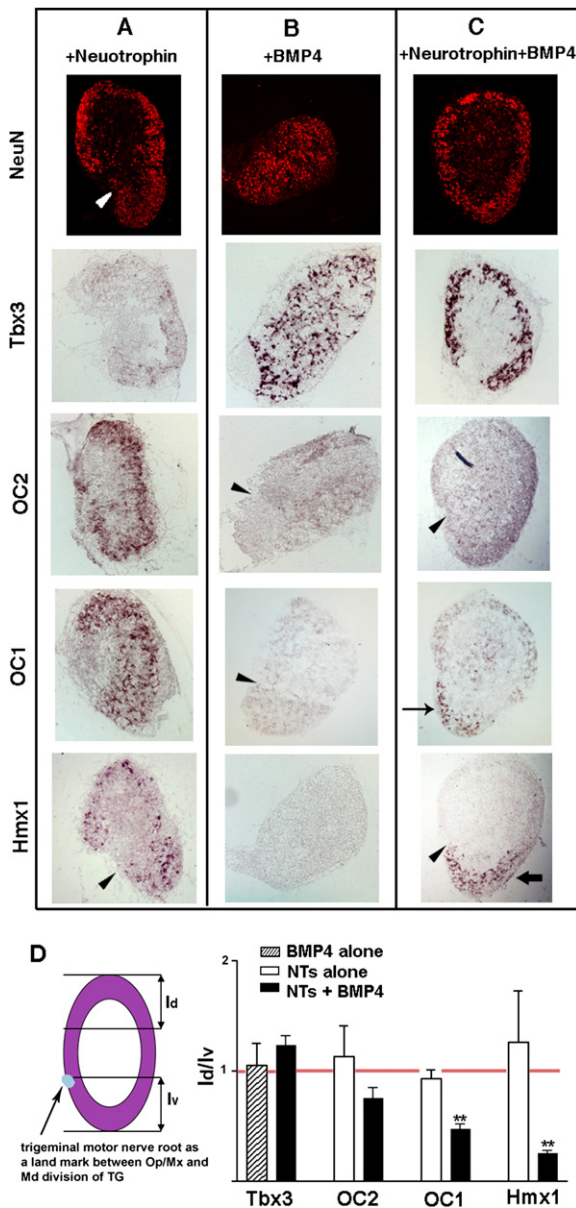
Figure 2. BMP4 Can Regulate the Expression Patterns of Four Transcription Factors in Cultured Trigeminal Neurons

(A–C) Isolated E11.5 trigeminal ganglia were cultured alone in medium with different supplements for 20 hr. Each ganglion was serial sectioned onto different slides and analyzed for the expression of NeuN (antibody), *Tbx3*, *OC2*, *OC1*, and *Hmx1* (in situ hybridization). NeuN expression labels neurons but not neural progenitor or glial cells in the culture. (A) Medium supplemented with 50 ng/ml NGF and 50 ng/ml NT3. (B) Medium supplemented with 20 ng/ml BMP4 alone. (C) Medium supplemented with 50 ng/ml NGF, 50 ng/ml NT3, and 20 ng/ml BMP4. Arrowheads point to the position of trigeminal motor root that is positioned between maxillary and mandibular division of TG. Arrow points to high *OC1* expressing neurons, and block arrow indicates *Hmx1* expressing neurons in the mandibular division of TG.

(D) Spatial differences of in situ signal intensities are examined by measuring the average signal intensity in the dorsal one-third (Id) and that in the ventral one-third (Iv) of the ganglion (illustrated by the scheme on

reduction in NT-dependent *OC2* and *OC1* expression, and an apparent mandibular specific expression of *Hmx1* (Figure 2C and Table 1). The strongest *OC1*-expressing cells also appear to be in the mandibular part of the cultured TG. Quantitative analyses (Table 1, fourth column) of the in situ signals comparing dorsal one-third versus ventral one-third of TG (Id/Iv) confirm our observation that *OC1* (Id/Iv = 0.48) and *Hmx1* (Id/Iv = 0.25) are more highly expressed in the ventral than in the dorsal region of the TG.

Since the expression levels of these transcription factors are not uniform across the ganglia under this culture condition, for simplicity, we measured the maximum (i.e., the strongest) in situ intensities. We found that BMP4 plus NTs caused a 10-fold increase in the expression of *Tbx3*, a 50% reduction in the *OC2*, and a mild inhibition of *OC1* and *Hmx1* levels in the mandibular neurons (Table 1). BMP4 alone is sufficient to induce *Tbx3* expression, although the level is weaker than that induced by BMP4 plus NTs (Figure 2B and Table 1, second column). Our results indicate that TG neurons have intrinsic differences that allow them to respond to extrinsic BMP4 differentially. Ophthalmic and maxillary neurons are very responsive to BMP4-mediated suppression of *OC1* and *Hmx1*, while mandibular neurons are refractory to such suppression. On the other hand, BMP4 induces *Tbx3* expression to similar levels in almost all TG neurons, suggesting that the intrinsic differences in responses to BMP signaling do not involve all genes but are specific to a specific subset. As a control for the specificity of BMP4, we found that neither BMP7 nor ActivinA at a concentration of 20 ng/ml had any obvious effect on the expression of these transcription factors (Figure S4 for BMP7 and data not shown for ActivinA).

Bmp4 and Phosphorylated-SMAD1/5/8 Expression In Vivo

The results from the in vitro experiments with BMP4 prompted us to investigate the in vivo expression pattern of *Bmp4* by utilizing the *Bmp4^LacZ* mouse in which the *LacZ* gene is inserted into the *Bmp4* locus as a reporter (Furuta and Hogan, 1998; Lawson et al., 1999). At E9.5, *Bmp4* is expressed in the optic cup and in ectodermal tissues at the distal regions of the first branchial arch, which are not in contact with the ganglion (Figure S5A). At E10.5, comparing the whole-mount LacZ staining to the whole-mount neurofilament (NFM) staining of *Bmp4^LacZ* embryos (littermates), it is apparent that at this stage, some ophthalmic and maxillary trigeminal axons are in contact with *Bmp4* expressing cells, while mandibular axons are not (Figure 3A). For E11.5 embryos, we costained tissue sections with β-gal (for *Bmp4*) and anti-NFM antibodies

the left) in NeuN-positive regions (represented by the purple color in the scheme). The ratio of Id/Iv for different genes under different culture conditions is shown in the graph. Red line is ratio = 1.0, i.e., equal intensity. **p < 0.01. Error bar represents SEM.
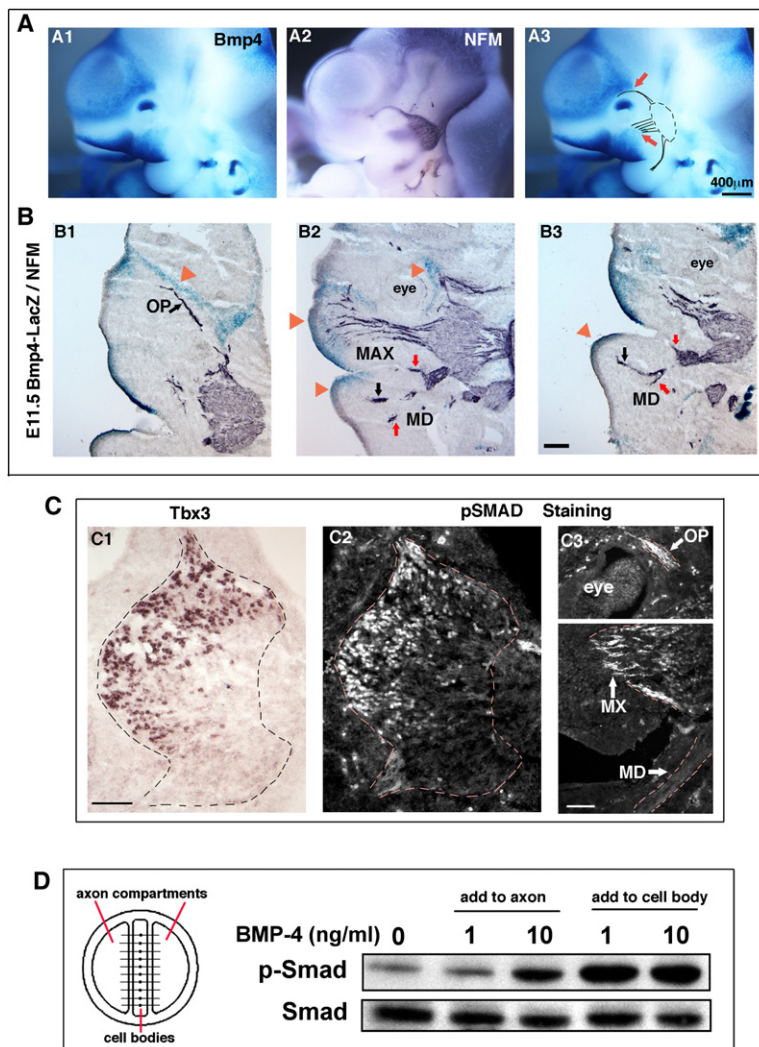
Figure 3. BMP4 Expression in Specific Craniofacial Regions and BMP Signaling in Trigeminal Neurons

(A) Comparison of the whole-mount LacZ staining of an E10.5 *Bmp4-LacZ* embryo (A1) and the whole-mount neurofilament staining of a littermate (A2) indicates that Bmp4 is expressed in regions adjacent to ophthalmic and maxillary axons (red arrows [A3]).

(B) Spatial distribution of Bmp4 expression and its relation with the growing trigeminal peripheral axons at E11.5. LacZ staining (blue color) reports where *Bmp4* is expressed, while NFM staining (purple color) shows the projection of trigeminal axons. Orange arrowheads point to *Bmp4* expressing areas. OP, ophthalmic axons; Max, maxillary axons; MD, mandibular axons. Black arrows point to a subpopulation of mandibular axons that project toward a small region where *Bmp4* is expressed, while red arrows point to mandibular axons projecting to regions where *Bmp4* is not expressed. Scale bar for each row is the same, 100 μm.

(C) Phosphorylated-Smad1/5/8 (pSmad) staining in an early E11 (Theiler stage 18) embryo. Adjacent sagittal sections were analyzed either for the expression of *Tbx3* by in situ hybridization (C1) or for the signal of pSmad by immunofluorescence (C2 and C3). The three trigeminal peripheral nerves are outlined in (C3). Scale bar is 50 μm.

(D) Trigeminal neurons were cultured in compartmented chambers and treated with BMP4 (1 or 10 ng/ml) for 2 hr by adding BMP4 to either the cell body or the distal axon chambers. Lysates of the cell body compartment were then immunoblotted with an antibody specific for pSmad1/5/8 or Smad1/5/8.

(to reveal the trigeminal axons; Figure 3B). At this stage, *Bmp4* is expressed in regions adjacent to the ophthalmic axons (Figure 3B1), and in the distal half of the maxillary arch into which many maxillary axons have grown (Figure 3B2). In the mandibular arch, *Bmp4* is restricted to only the dorsal and distal-most ridges toward which only a small population of mandibular axons projects (Figure 3B3). The spatial distribution of *Bmp4* mRNA puts BMP4 in an excellent position to induce *Tbx3* and to suppress *OC2*, *OC1*, and *Hmx1* transcription in the ophthalmic and the maxillary trigeminal neurons in early development. Other *Bmp* family members are either not expressed or weakly expressed (such as *Bmp7*) at these stages (Figure S5B and data not shown).

A hallmark of canonical BMP4 signal transduction is the phosphorylation of Smad-family transcription factors, in particular Smad1/5/8 (Massagué and Gomis, 2006; Nohe et al., 2004). We therefore performed anti-phosphoSmad1/5/8 staining (hereafter referred to as pSmad staining) in fixed embryos. pSmad-positive cells (nuclei)

are located in the ophthalmic and dorsal maxillary domains of the TG (at E11), but not in the mandibular division (Figure 3C2). In situ hybridization of adjacent sections demonstrates that the *Tbx3* pattern is almost identical to that of the pSmad staining (Figure 3C1). These results confirm the existence of position-dependent BMP signaling within the TG in vivo. They also suggest that *Tbx3* is likely to be a direct transcriptional target of BMP signaling in neurons, a finding consistent with previous reports in other systems (Yang et al., 2006).

BMP4 Can Signal to Trigeminal Neurons in a Retrograde Manner

The pattern of nuclear pSmad in regions of the trigeminal ganglion correlates very well with where the trigeminal axons are in contact with *Bmp4* expressing cells in peripheral targets, suggesting that BMP4 signals to these neurons in a retrograde manner, from axons to cell bodies. To directly test this possibility, we performed compartmentalized cultures of TG neurons using Campenot

chambers (Campenot, 1982). We found that 10 ng/ml of BMP4 added only to the distal axons can indeed significantly increase the amount of pSmad in the cell bodies as examined by Western blot (Figure 3D). Interestingly, intense pSmad staining was seen in the axons of ophthalmic and maxillary neurons but not in mandibular axons (Figure 3C3). Therefore, phosphorylated-Smads themselves could, in principle, be the retrograde messenger that are transported back to the cell bodies and then imported into the nuclei to induce transcriptional changes, a hypothesis that needs to be tested by future experiments.

BMP4 Is a Major Target-Derived Factor Regulating the Expression of Positional Identity Genes in Trigeminal Neurons In Vivo

The results described above predict that in vivo deficiency in *Bmp4* should disrupt the expression patterns of positional identity markers in trigeminal neurons. *Bmp4* null mouse mutants are early embryonic lethal (Dunn et al., 1997). In the outbred ICR background, some of the null embryos can survive up to early E10.5. We performed expression analyses at approximately E10.25 (prior to death) in mutant and stage-matched heterozygous embryos. In the heterozygous controls, pSmad staining and strong expression of *Tbx3* can be seen in a few scattered cells in the ophthalmic and dorsal part of the maxillary TG. There is also a weak *Tbx3* expression throughout the ganglion (Figure 4A). In contrast, in *Bmp4* null mutant, pSmad staining is completely absent, and no strong *Tbx3* expression is observed (Figure 4B). The differences are not due to the compromised viability or failed differentiation of neurons as NFM staining can be clearly visualized in TG neurons in *Bmp4* null embryos (Figure 4B). Moreover, in culture, TG isolated from *Bmp4* null embryo are as competent in turning on *Tbx3* expression as TG from Bmp4$^{+/-}$ embryos (Figure S6). Taken together, our results strongly support the hypothesis that BMP4 is the major target-derived factor that activates Smad1/5/8 and induces *Tbx3* in TG neurons at this stage in vivo.

The spatially restricted patterns of *OC1* and *OC2* have not yet been established at this point in control embryos (Figure 4A). However, the levels of *OC2* and *OC1* do appear mildly increased in *Bmp4* mutant embryos, consistent with a model in which BMP4 normally suppresses their expression as observed in vitro (Figure 4, compare lower panels with upper panels). The localization of *Hmx1* transcripts is still confined to the mandibular region in *Bmp4 null* embryos, suggesting that this restricted pattern can be established by factors other than BMP4 at this stage (Figure 4B). This result, however, does not rule out a role of BMP4 in maintaining the mandibular restricted expression of *Hmx1* at later stages such as E11.5.

Analyses of *Smad4*-Deficient Trigeminal Ganglia Neurons

To further analyze the retrograde BMP4 signaling from the perspective of TG neurons, we took advantage of two transgenic mouse lines: Wnt1-Cre and floxed-Smad4 (*Smad4^C*) mice. Wnt1-Cre mice express Cre recombinase in neural crest cells including precursors to trigeminal neurons as well as cells populating the branchial arches (Chai et al., 2000; Jiang et al., 2000). *Smad4^C* is a conditional (loxP-flanked) mutant allele of the *Smad4* gene (Li et al., 2003; Yang et al., 2002). Smad4 is the common Smad protein (co-SMAD) mediating signaling downstream of TGFβ family factors (including BMPs). It binds to the phosphorylated R-Smad proteins (Smad1//5/8 for the BMP pathway), and the resulting complex is translocated into the nucleus to induce gene expression changes (Massague and Gomis, 2006; Nohe et al., 2004). We examined embryos that are homozygous for the floxed-Smad4 allele (*Smad4$^{C/C}$*) and also carry the Wnt1-Cre transgene (designated as Smad4-CKO, for Smad4 conditional knockout).

The Smad4-CKO embryos do not survive beyond E12.5 due to heart defects (Liu et al., 2004; Stottmann et al., 2004; data not shown). Thus, we analyzed TG at E11.5. As revealed by NFM and NeuN staining, the size of the TG and the total number of TG neurons in the Smad4-CKO embryos are less than 40% of those for control ganglia from *Smad4$^{C/C}$* without Cre or (*Smad4$^{C/+}$; Wnt1-Cre*) embryos (NFM staining shown in Figures 4C and 4D, NeuN staining in Figure S7A and Table 2). NFM staining revealed a dramatic defect in peripheral projections from TG neurons in the Smad4-CKO embryos (Figure 4D). Instead of one maxillary branch, two bundles are formed in the mutant: a dorsal (d-Mx) and a ventral (v-Mx) maxillary nerve. The v-Mx (arrowhead in Figure 4D) and the mandibular nerve (arrow in Figure 4D) are tangled together, largely stopping at the boundary between the maxillary and mandibular arches. The ophthalmic and d-Mx axons are able to extend toward the eye or into the maxillary arch, respectively, but they do not extend all the way into the peripheral tissues to form branches (Figure 4D1).

Although at present we do not know the molecular mechanisms underlying these abnormal peripheral axon projections in the Smad4-CKO embryos, we can take advantage of the phenotype to test the BMP-retrograde signaling hypothesis. The misprojection of the ventral maxillary (v-Mx) neurons should prevent them from receiving the BMP4 signal derived from the distal part of the maxillary arch (Figures 3A and 3B), and as expected, pSmad1/5/8 signal is significantly reduced in the v-Mx part of TG in Smad4-CKO embryos (Figure 4F, arrow). We quantified the average pSmad1/5/8 intensity in each of the three TG divisions separately. The average pSmad signal in the ophthalmic region (Op-pSmad) in control *Smad4$^{C/C}$* embryos was assigned as 100%. Similar levels of pSmad staining are present in ophthalmic and maxillary (Mx-pSmad) divisions in control E11.5 TG (Figures 4E and 4F; Table 2). In contrast, in the Smad4-CKO TG, there is a mild reduction in Op-pSmad (78% of the control Op-pSmad), and a dramatic reduction in Mx-pSmad level (44% of the control; Table 2).

Next, we examined the spatial patterns of the four genes in Smad4-CKO TG. Compared with the results
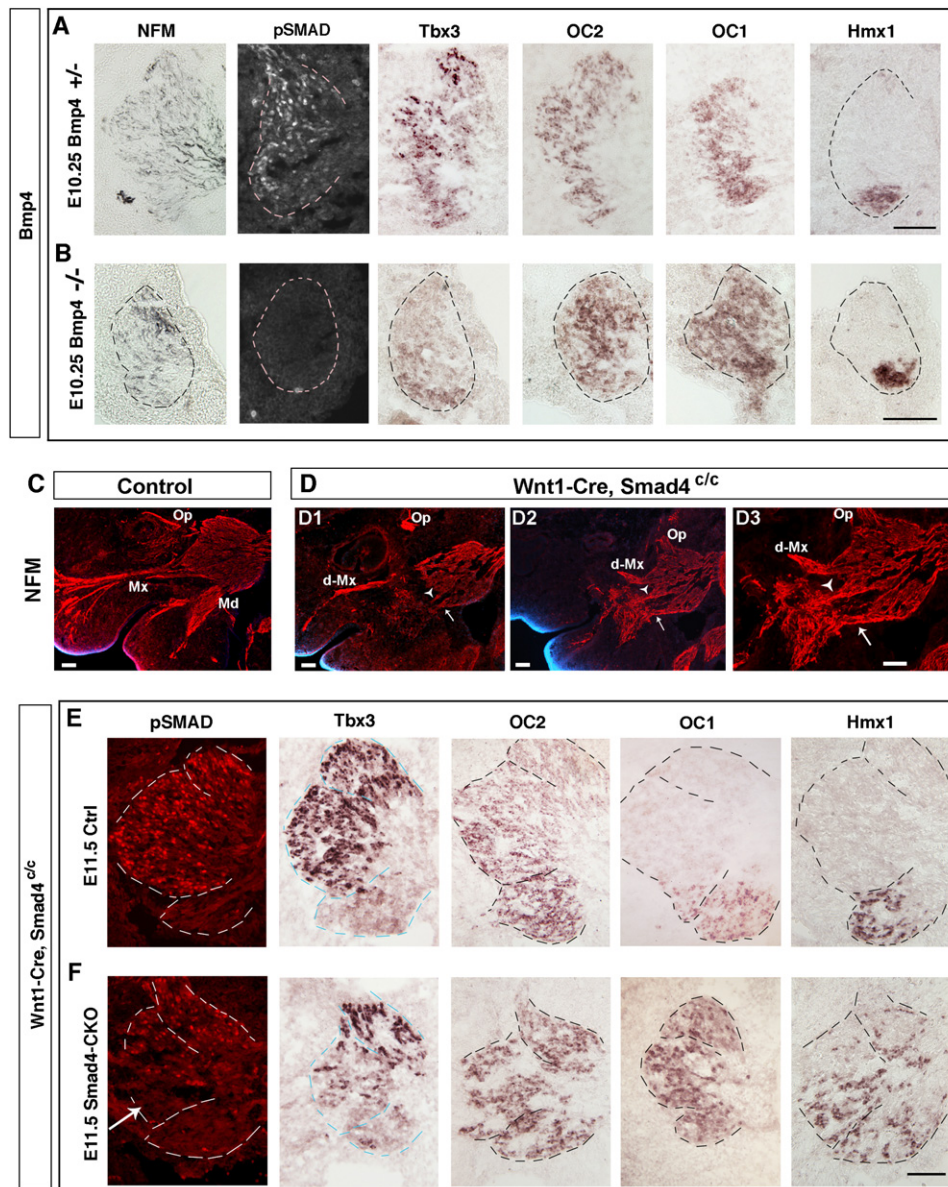
Figure 4. Altered Spatial Patterns of Positional Identity Markers in *Bmp4* Null and *Smad4* Conditional-Deletion Embryos

(A and B) Stage-matched E10.25 *Bmp4* heterozygous +/− (A) or homozygous −/− (B) embryos were serial sectioned and analyzed for the expression of neurofilament (NFM, by immunohistochemistry), pSmad (by immunofluorescence), and *Tbx3*, *OC2*, *OC1*, *Hmx1* (all by in situ hybridization). Note the lack of strong *Tbx3* and pSmad signals in *Bmp4* null embryos. Scale bar for each row is the same, 100 μm.

(C and D) Neurofilament (NFM) staining in E11.5 Smad4$^{c/c}$ ([C], control) or Wnt1-Cre; Smad4$^{c/c}$ ([D], Smad4-CKO) embryos. In Smad4-CKO mice, two axon bundles grew from the maxillary division: a dorsal branch (d-Mx) and a ventral branch (arrowhead). The ventral maxillary axons and the mandibular axons (arrow) are tangled together and largely stop at the border between the maxillary and mandibular arches. (D3) is an enlarged photo of (D2). The d-Mx and Op branches do project into periphery in the mutant. Red is NFM, blue is DAPI. Scale bar is 100 μm.

(E and F) E11.5 Smad4$^{c/c}$ ([C], control) or Wnt1-Cre; Smad4$^{c/c}$ ([D], Smad4-CKO) embryos were serial sectioned and analyzed for the expression of pSmad, *Tbx3*, *OC2*, *OC1*, and *Hmx1*. Arrow points to the lack of pSmad staining in the ventral maxillary division of TG in mutant. The dashed lines roughly delineate the three trigeminal divisions. Scale bar for all pictures in (C) and (D) is the same, 100 μm.

from controls, in Smad4-CKO embryos (at E11.5), *Tbx3* is expressed in very few cells in the maxillary region of the TG but is still transcribed in many cells in the ophthalmic division. *OC2* is almost uniformly expressed throughout the TG as opposed to the graded pattern in the control ganglion. *OC1* is also transcribed throughout the TG in mutant. Finally, *Hmx1* expression is expanded into the ventral maxillary TG and also appears in a few cells in the ophthalmic region, in contrast to its mandibular restricted distribution in control embryos (Figures 4E and

Table 2. Quantitative Analyses of Smad4 Conditional Mutant Trigeminal Ganglia

		Control (Smad4$^{C/C}$)	Smad4-CKO (Wnt1Cre;Smad4$^{C/C}$)
Total number of NeuN-positive cells		22837 ± 1158	8321 ± 677**
Spatial index of pSMAD intensity (relative average intensity among TG divisions)	Op-pSMAD	100% ± 6.0%	78.3% ± 10.4%*
	Mx-pSMAD	105.9% ± 14.4%	44.5% ± 10.6%**
	Md-pSMAD	45.1% ± 7.7%	40.8% ± 4.1%
% of NeuN-positive cells expressing marker (in the entire TG)	Tbx3/NeuN$^+$	55.3% ± 3.0%	12.0% ± 1.5%**
	Hmx1/NeuN$^+$	15.1% ± 3.0%	22.6% ± 2.8%*
Relative in situ intensity in the *maxillary* TG	Tbx3-Mx	100% ± 3.8%	24.3% ± 3.6%**
	Hmx1-Mx	100% ± 5.6%	1742.8% ± 213.2%**
Spatial index of OC1 and OC2 in situ intensity (dorsal TG/ventral TG)	OC1-Id/Iv	0.18 ± 0.03	0.69 ± 0.07**
	OC2-Id/Iv	0.41 ± 0.03	0.95 ± 0.03**

Six control and six mutant trigeminal ganglia are quantified. Statistical analyses were performed comparing the results from Smad4-CKO with those from control embryos. *p < 0.05; **p < 0.01.

4F; Table 2). These results strongly support our BMP-retrograde signaling hypothesis, because in the maxillary TG where pSmad1/5/8 is most severely reduced in Smad4-CKO mutants, we observe the most dramatic changes in the expression of the candidate positional markers (also see Table 2). The *Hmx1* result indicates that BMP signaling, although dispensable for initiating the mandibular specific *Hmx1* expression (Figure 4B), is important for maintaining this spatial pattern, a finding very similar to the in vitro effect of BMP4 on *Hmx1* expression in cultured TG (Figure 2C).

Wnt1-Cre should mediate the deletion of *Smad4* in almost all of TG neurons in the conditional mutant, yet in ophthalmic and dorsal maxillary TG where many neurons receive BMP signal (judged by pSmad1/5/8), we still observed strong *Tbx3* expression and *Hmx1* suppression (see Table 2 for total number of NeuN$^+$ cells expressing *Tbx3* or *Hmx1*). These results raise the possibility that *Tbx3* and *Hmx1* are regulated by Smad4-independent (but Smad1/5/8-dependent) BMP signaling. To test this, we turned again to in vitro culture experiments. In the presence of BMP4 and neurotrophins (NTs), TG isolated from Smad4-CKO were as responsive in turning on *Tbx3* expression throughout the ganglia as the control TG and were also able to largely restrict *Hmx1* transcription to mandibular regions with rare exceptions (Figures S7B–S7D). Therefore, Smad4 is not required in TG neurons for mediating the effects of BMP4 on *Tbx3* and *Hmx1*. In contrast, in the same culture (BMP4 plus NTs), Smad4 mutant TG expressed much higher levels of *OC2* and *OC1* than the control TG (Figures S7B and S7C), suggesting that suppressing the expression of these two genes by BMP4 *does* require Smad4, at least under this culture conditions.

Taken together with the results from *Bmp4* mutant embryos, our studies strongly support the hypothesis that the positional differences in gene expressions are largely

a consequence of differential retrograde BMP4 signaling. Trigeminal neurons that contact BMP4-producing regions on the face acquire specific gene expression profiles (i.e., strongly induced *Tbx3*, reduced *OC2*, suppressed *OC1*, and continued absence of *Hmx1* expression). This is achieved during the process of peripheral innervation through activation of pSmad-mediated transcriptional programs that are either Smad4-dependent or Smad4-independent.

Defects in Whisker Maps Formed by OC2-Deficient Trigeminal Neurons

Trigeminal central axons innervate the CNS and form synapses much later after the peripheral axons have selected specific craniofacial targets. We therefore hypothesize that these peripheral target-induced gene expression changes are used to regulate the central projections so that facial structures can be precisely mapped onto the brainstem. Because *Bmp4* null mutants, as well as Smad4-CKO embryos, die before the projection of trigeminal central axon-collaterals into the hindbrain, we cannot study the face maps formed in these embryos. However, mice lacking *OC2*, one of the positional identity genes regulated by BMP4, are viable (Clotman et al., 2005), allowing us to test our hypothesis in these mice. *OC2* is not expressed in the craniofacial organs (Figure S8) or in any of the brainstem trigeminal nuclei that are the central targets of TG neurons throughout development (Figure 5B). Therefore, the lack of *OC2* should only affect TG neurons themselves. Consistent with this, the peripheral projections of trigeminal axons are normal in *OC2* mutant embryos (Figure S8), and we found no difference in the numbers of large and small whiskers in all genotypes (data not shown). Moreover, the size of *OC2* mutant TG and the number of TG neurons are not statistically different from the controls (data not shown).
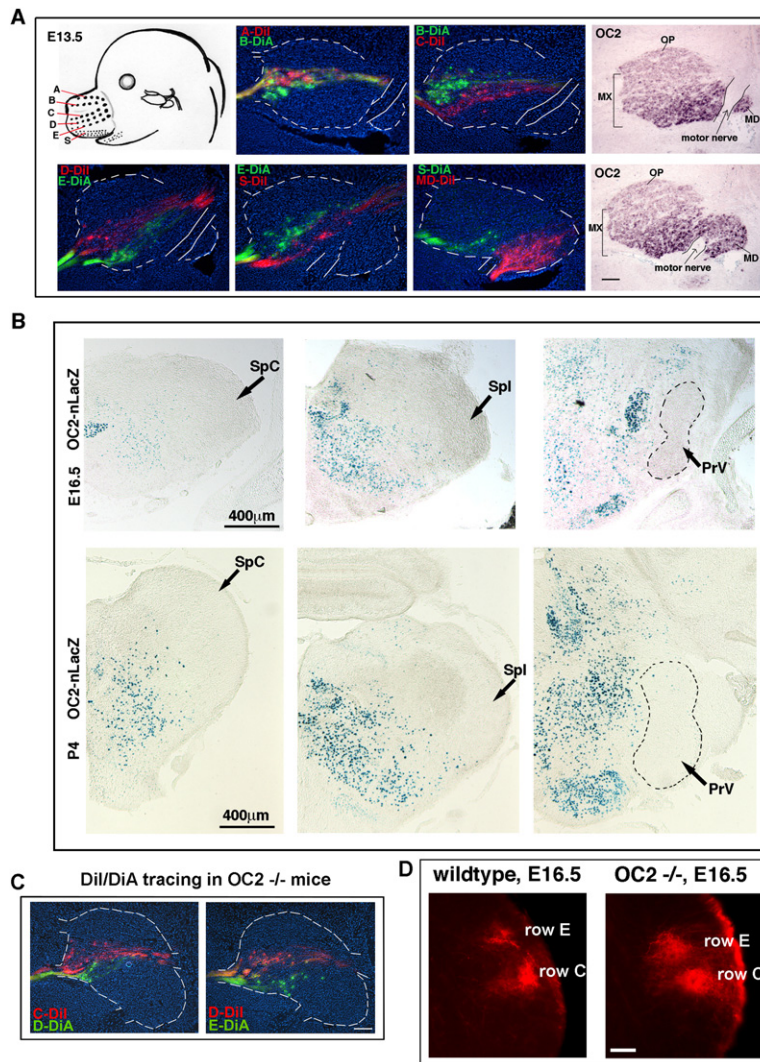
Figure 5. *OC2* Expression and Coarse Topographic Axon Orders in *OC2* Mutant

(A) Retrograde dye tracing demonstrates that high-*OC2*-expressing neurons in the maxillary division of the trigeminal ganglion correlate with those that innervate large whisker rows C, D, E and small whiskers (S) on the face. DiI/DiA crystals were injected into adjacent rows (see schematic drawing) to retrogradely label trigeminal neuron cell bodies in E13.5 embryos. Representative tracing results are provided for each case. Sections hybridized to the *OC2* in situ probe are also shown in the rightmost panels. The trigeminal motor nerve (outlined by solid lines) projects through the ganglion and separates the mandibular division from the ophthalmic and maxillary divisions. Scale bars are 100 μm.

(B) The absence of *OC2* expression in the central trigeminal nuclei indicated by LacZ staining in *OC2*-nLacZ heterozygous mice. The targeted mutation of the *OC2* gene replaced exon 1 with nuclear LacZ gene. Thus, in *OC2-nlacZ* heterozygous mice, LacZ staining is a reporter for *OC2* expression. LacZ staining is *absent* in the central trigeminal nuclei: SpC (*Caudalis*), SpI (*Interpolaris*), and PrV (the principle trigeminal nucleus, outlined in the figure). Two developmental stages were shown (E16.5 and P4).

(C) Two-color DiI/DiA tracing from whisker rows C/D or D/E in *OC2* mutant mice showed that the cell bodies of neurons innervating rows C, D, and E are still segregated within the ganglia similar to the controls shown in (A). Scale bar is 100 μm.

(D) Retrograde DiI tracing from whisker row C and row E demonstrates that the coarse topography of trigeminal axon projections into the brainstem is maintained, although the labeling appears to be more diffused in *OC2* mutant. Scale bar is 100 μm.

OC2 Is Expressed at a Higher Level in Trigeminal Neurons Innervating Ventral Whiskers

OC2 expression is low in the dorsal part of TG, while it is highly expressed in the ventral part of TG (Figures 1G, 1H, and 5A). To correlate these two domains with the peripheral innervation of TG neurons, we performed retrograde dye tracing experiments. We placed DiI and DiA crystals into adjacent rows of embryonic whiskers (rows A–E for large whiskers, S for small whiskers, as illustrated in Figure 5A). Comparing of the DiI/DiA tracing results with the *OC2* in situ hybridization results (Figure 5A), it appears that rows A and B are likely innervated by low-*OC2* expressing neurons, whereas rows D, E, and S (small whiskers) are probably innervated by high-*OC2* expressing cells; row C is supplied by neurons at the boundary of the two domains. Thus, the lack of *OC2* expression should predominantly affect the central representation of the whisker rows of C, D, E, and S.

Topographic Axonal Order Is Largely Maintained, but Defects Are Observed in the Fine Whisker Maps Formed in OC2 Mutant Mice

To examine the approximate topographic order of trigeminal central projections, DiI crystals were placed into whisker rows C and E of fixed E16.5 embryos for anterograde axon tracing. Two segregated clusters of axon termini within the brainstem were labeled in both control and *OC2* mutant (Figure 5D), suggesting the coarse topographic order of TG axons was maintained in *OC2* null animals. However, the labeled clusters in the mutant brain appeared wider, the distance between the two clusters were narrower, and some diffuse labeling was seen (Figure 5D), suggesting there are subtle mistakes or positional shifts in axonal projections. The more diffused central projections are not a consequence of mispositioned cell bodies in the TG. In the *OC2* mutant TG, neurons innervating rows C, D, and E are still well segregated (Figure 5C).

Since DiI tracing results are of low resolution and highly variable, we turned to cytochrome oxidase (CO) staining for a better assessment of the whisker maps. The overall pattern of five rows of large barrelettes is preserved in the *OC2* mutant (Figure 6A). However, there are variably misaligned barrelettes and fused barrelettes in all the *OC2* mutant animals examined (n = 10, arrows in Figure 6A). In addition, the small barrelettes (depicted by dashed lines) that represent small whiskers around the lips were poorly formed, as the boundaries between individual small barrelettes were largely blurred (Figures 6A–6C). The number of clearly defined small barrelettes in OC2 mutant is about half of the number in control animals (Figure 6C) even though the number of small whiskers on the face are the same in all genotypes. This defect is observed in both the spinal interpolaris nuclei SpI (Figure 6A) and the principle trigeminal nuclei PrV (Figure 6B). Furthermore, the total area of barrelettes representing rows C, D, and E (Area$_{CDE}$) is smaller in *OC2* mutant mice whereas the barrelettes area representing rows A and B (Area$_{AB}$) is largely unchanged (Figure 6D). The average ratio of Area$_{CDE}$:Area$_{AB}$ is 1.7 in control (heterozygous and wild-type) animals, whereas it is reduced to an average of 1.2 in mutants (Figure 6E; p < 0.01). These results are consistent with the idea that ventral trigeminal neurons are more defective than dorsal trigeminal neurons in mapping whiskers onto the brain in *OC2* mutant mice.

Taken together, the analyses on the *OC2* mutant phenotype support the hypothesis that the graded expression of *OC2,* induced by target derived BMP4, is necessary to instruct the fine mapping of whiskers by trigeminal central axons. The defects in *OC2* mutants are clear, though relatively mild, presumably because other transcription factor genes (*Tbx3*, *OC1*, and *Hmx1*) which are expressed normally in the *OC2* mutant TG (Figure S8C), also contribute to patterning the central projections.

DISCUSSION

We have identified a set of candidate "positional identity" labels for mouse trigeminal sensory neurons that innervate and represent discrete areas of the rodent's face. We present evidence that after initial axonal outgrowth, peripheral target-derived signals can regulate gene expression in trigeminal neurons through a retrograde signaling mechanism. BMP4 is one such factor released by craniofacial tissues that patterns trigeminal neurons. Support for this idea comes from several different experiments, including in vitro culture assays, the in vivo correlation between the *Bmp4* expression pattern and the spatial distribution of phosphorylated-Smad1/5/8 in trigeminal neurons, and the analysis of both *Bmp4* null mutant and Smad4-CKO embryos. This retrograde regulation of positional differences operates while the trigeminal peripheral axons are in the dynamic process of innervating the craniofacial targets. We hypothesize that this mechanism allows the targets to communicate with the neurons about "what and where they are innervating." Consequently,
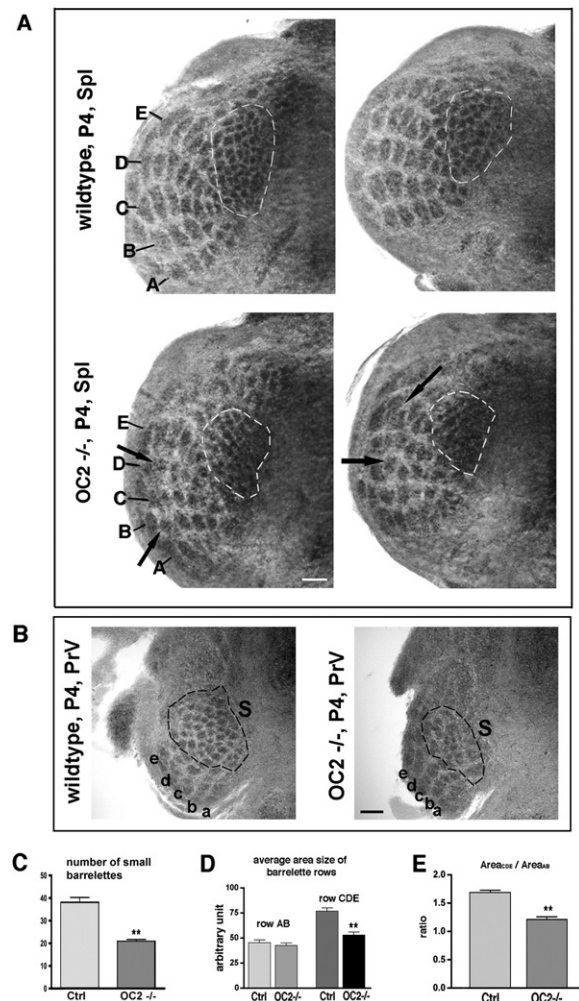
Figure 6. Whisker Maps Formed in the Brainstem Show Abnormalities in *OC2* Mutant Neonatal Mice

(A) Representative images of cytochrome oxidase staining in the brainstem nucleus *Interpolaris* from two different wild-type and two *OC2* homozygous mutant neonatal mice (P4, postnatal day 4). Dotted lines delineate the small barrelettes representing small maxillary whiskers on the upper lip. The five rows representing large whiskers are designated as A–E. Arrows point to the misaligned and fused barrelettes in *OC2* mutants. Scale bars are 100 μm.

(B) Representative images of cytochrome oxidase staining in the principle trigeminal nucleus (PrV) from wild-type and *OC2*$^{-/-}$ mutant mice. The large barrelette rows are designated as a–e. The small whiskers are circled together by a dotted line and designated as S. Scale bar is 100 μm.

(C) Number of small maxillary barrelettes. Error bars represent SEM. **p < 0.01, t test.

(D) Average total area size of barrelettes representing whisker rows of A and B (Area$_{AB}$), or rows C, D, and E (Area$_{CDE}$) is shown in the graph as arbitrary unit. Error bars represent SEM. **p < 0.01, t test.

(E) The ratio between the total area of row C, D, and E barrelettes (Area$_{CDE}$) and the total area of row A and B barrelettes (Area$_{AB}$) is reduced in *OC2* mutant mice. The average values of ACDE/AAB are 1.7 in controls (n = 10) and 1.2 (n = 9). Error bars represent SEM. **p < 0.01, t test.

neurons can use this information to make accurate central projections. Our examination of the face/whisker maps formed in the *OC2* mutant mice supports this hypothesis.

Spatial Patterning of Trigeminal Ganglia before the Onset of Axon Outgrowth

Trigeminal neurons are generated from both neural crest and neurogenic placode cells. The former originate from two specific segments of rhombomeres: r1 and r2 (Ayer-Le Lievre and Le Douarin, 1982) while the latter are also from two spatially distinct regions: the ophthalmic and maxillomandibular placodes (Begbie et al., 2002). Thus, precursor cells from different spatial regions may be prepatterned to populate only one of the three trigeminal divisions. Previous work in chick demonstrated that the *Pax3* gene is specifically expressed in the ophthalmic placode and *Pax3* positive cells are committed to become only the ophthalmic neurons (Baker et al., 1999). In our studies, we found that *Hmx1* expression is restricted to the ventral region of the trigeminal ganglion as early as E9.5 when the ganglion is just being formed (data not shown), supporting the idea that precursor cells are spatially patterned. This prepatterning is likely important for setting up the general somatotopic organization of the trigeminal pathways.

Cell-Fate Plasticity and Retrograde Regulation of Sensory Neuron Gene Expressions In Vivo after Peripheral Innervation

The spatial prepatterning in dividing precursor cells is not irreversible (at least at early stages). When *Pax3*-positive placodal cells are transplanted to trunk regions, they can be integrated into the DRG, innervate the body, and make appropriate central connections (Baker et al., 2002). In our studies, we showed that in vivo, BMP4 protein expressed in certain facial areas signals to trigeminal neurons in a retrograde manner to induce further gene expression changes as well as maintain the mandibular specific *Hmx1* expression (Figures 3 and 4). In Smad4-CKO mutant, v-Mx neurons that failed to receive BMP signal turned on *Hmx1* ectopically (Figure 4F). Similar "cell-fate plasticity" has been observed in young DRG neurons. In experiments using early chick embryos (chick embryonic day E2.5) when the dorsal half of the neural tube was surgically rotated such that the rostrocaudal order of DRGs, but not that of motoneurons, was reversed, sensory neurons grew axons into the body locations according to their "new" position (Wang and Scott, 1997, 1999).

Retrograde Signaling as a General Principle for Organizing Somatosensory as Well as Other Neural Circuits

Why then does the somatosensory system allow cell fate plasticity if there already exists a predetermined general somatotopy, as just described? We speculate that it may be related to the primary function of the somatosensory system: to precisely map the body. Each somatic sensory neuron has two axons: an axon that supplies a peripheral organ, and a central axon that sprouts a set

of collaterals that form synapses with second-order CNS neurons. The central collaterals always develop much later than the peripheral axons, perhaps waiting for the confirmation/information on "what and where are the targets on the body." In this way, even if a peripheral axon misprojects, the "new" target will be able to induce transcriptional changes in this neuron to guide its central axons to project accordingly. Indeed, experiments creating artificial "mistakes" have been performed with DRG neurons in frogs and chick. When thoracic cutaneous sensory afferents were surgically redirected to project along the brachial nerve into the forelimb of a chick embryo or a tadpole, not only did these axons supply the muscle spindles, they also formed synaptic connections with appropriate forelimb motoneurons that were not their original central partners (Ritter and Frank, 1999; Wenner and Frank, 1995). In the trigeminal system, target-derived BMP4 induces spatial differences in TG sensory neurons, and such molecular differences are important for TG neurons to map the face onto the CNS. This is supported by results obtained in mice deficient in one of the BMP regulated transcription factors, OC2. In particular, the small whiskers, normally innervated by high-OC2-expressing TG neurons, are not mapped properly onto the brainstem nuclei in *OC2* mutant mice (Figure 6).

Retrograde signaling has emerged as a widely used mechanism during the development of the nervous system in both vertebrate and invertebrate. Many studies have demonstrated that retrograde signaling by target-derived factors regulates neuronal survival, axon extension, axon branching, dendritic patterning, neurotransmitter phenotypes, as well as the synaptogenesis (reviewed in Frank and Wenner, 1993; Glebova and Ginty, 2005; Hippenmeyer et al., 2004; Howe and Mobley, 2005; Keshishian and Kim, 2004).

Role of Smad4 in Trigeminal Sensory Neuron Development

Our analyses of the Wnt1-Cre-mediated Smad4 conditional knockout (Smad4-CKO) embryos revealed several interesting phenotypes. Major defects occurred in the peripheral axonal projections of trigeminal neurons, the most obvious one being the entanglement of the v-Mx axons with the mandibular axons (Figure 4D). The aberrant axonal projections prevent the neurons in the v-Mx TG from receiving BMP signaling as indicated by a significant reduction of the pSmad1/5/8 signal (Figure 4F). It also results in changes in the expression of the four transcription factors (Figure 4F and Table 2), therefore strongly supporting our hypothesis that target-derived BMP signaling regulates spatial patterns of gene expression in TG.

Using in vitro cultures, we found that Smad4 is largely dispensable for BMP regulated *Tbx3* and *Hmx1* expression (Figure S7), whereas it is required for maximum suppression of *OC2* and *OC1* transcription in TG neurons (Figure S7). The Smad4-independent regulation of *Tbx3* may be cell type specific. A previous study on heart and limb identified *Tbx3* as a direct target of BMP signaling

in these tissues, and showed that both Smad1 and Smad4 can activate the *Tbx3* promoter in vitro; therefore, although Smad4 is not necessary to induce *Tbx3*, it may be sufficient to do so. (Levy and Hill, 2005; Yang et al., 2006). Coexistence of Smad4-independent and Smad4-dependent Smads transcription complexes in response to BMP signaling may be a general phenomenon in many biological processes (Biondi et al., 2007; Chu et al., 2004).

Implications for Face Representation during Natural Selection, Variation, and Evolution

One potential advantage of allowing peripheral targets to influence the gene expression of trigeminal neurons is to give the sensory system the ability to make adaptive changes when the face/body changes during natural selection and variation. In our study, we showed that craniofacial derived BMP4 has a profound influence on gene expression in trigeminal neurons. It is interesting to note that BMP4 was recently suggested to be one of the key regulators of the morphological variation of beaks in Darwin's finches by both correlative expression studies in finch species and by experiments using chick embryos (Abzhanov et al., 2004; Wu et al., 2004). Together with our results, it implies that the same factor that regulates craniofacial morphological changes during natural selection also helps control sensory neuron gene expression. This would allow adaptive changes in facial structures to be immediately coordinated with and reflected by the trigeminal sensory system, thereby facilitating the coevolution of the two systems.

EXPERIMENTAL PROCEDURES

Mice

The generation and genotyping method of *Bmp4-lacZ* (Dunn et al., 1997), *Wnt1-Cre* (Jiang et al., 2000), *Smad4* conditional mutant (Li et al., 2003), and *OC2* mutant (Clotman et al., 2005) mice have been described previously.

Methods for Various Histological Analyses

In situ hybridization, anti-PGP9.5 staining, and cytochrome oxidase staining are performed according to methods previously described (Fundin et al., 1997; Graef et al., 2003; Li et al., 1994). For in situ hybridization and anti-NeuN costaining, in situ hybridization was carried out first, followed by incubation with anti-NeuN antibody (Chemicon) and detected by Alexa 568-labeled anti-mouse IgG (Invitrogen). For pSMAD staining, sections were incubated with Phospho-SMAD 1/5/8 (Cell Signaling) antibody at 37°C for 3 hr, followed by Alexa 488-conjugated secondary antibodies (Invitrogen). For LacZ and anti-Neurofilament costaining, sections of E11.5 embryos were developed in X-gal staining solution overnight and then stained with 2H3 antibody (Developmental Studies Hybridoma Bank). For lipophilic dye tracing, DiI or DiA crystals (Invitrogen) were injected into fixed embryos and allowed to diffuse at 37°C for 2 days for E10.5 embryos, 1 week for E13.5 embryos, and 8 to 12 weeks for E16.5 embryos. One hundred micrometer vibratome sections were collected and examined using a fluorescent microscope.

Neuronal Culture

Trigeminal ganglia were isolated and cultured in collagen matrix (UP State) as described previously (Graef et al., 2003). NT3 (50 ng/ml,

Peprotech Inc.), NGF (50 ng/ml, Sigma), recombinant human BMP4 (20 ng/ml, R&D Systems) were used as supplements. For compartmentalized cultures, trigeminal neurons were cultured on laminin (10 μg/ml) inside teflon chambers (Tyler Research) as described previously (Campenot, 1982). Either cell bodies or distal axons were exposed to BMP4 (1 or 10 ng/ml) for 2 hr before cell body lysates were collected. All lysates were gel separated (SDS-PAGE) and immunoblotted with an antibody against phosphorylated Smad1/5/8 (1:1000) and Smad1/5/8 (1:1000, Cell Signaling).

Quantitative Analyses Methods
Quantification of In Vitro Cultures

Each trigeminal ganglion is serial sectioned onto four slides such that the expression of the four transcription factors under each of the culture conditions within the same ganglion can be assessed simultaneously. In situ hybridization procedures were carried out completely in parallel for all culture conditions, followed by anti-NeuN staining on the same slides. Images of all sections were acquired using the same exposure time. Only NeuN-positive cells are quantified. In situ signal intensities were measured using Metamorph software and corrected for background. Three independent experiments were carried out, and the results were averaged; p values are calculated using Student's t test. For spatial expression differences, the ventral region/mandibular division was identified by the presence of the motor-root which formed a dent between the ophthalmic/maxillary and the mandibular divisions of the TG. Each ganglion was then oriented in the same direction. Every section from a trigeminal ganglion was arbitrarily divided into three divisions along the D-V axis of the ganglion (shown in Figure 2D). Average in situ intensities of dorsal one-third, and ventral one-third were measured using Metamorph software. Results from three ganglia were averaged.

Quantitative Analyses of Smad4-CKO and Littermate Control Embryos

The number of neurons were counted using the method described by Huang et al. (1999b). pSmad and in situ signal intensities were measured using Metamorph software. Six mutant and six control ganglia were measured, and the results were averaged and compared. p values are calculated using Student's t test.

Quantification of OC2 Mutant Phenotypes

After CO staining, images of all the hindbrain sections were acquired. The number of small barrelettes is counted blindly. The areas of the barrelettes rows are measured in Metamorph. The results from OC2 mutant mice were compared to wild-type and heterozygous controls. p values are calculated using Student's t test.

REFERENCES

Abzhanov, A., Protas, M., Grant, B.R., Grant, P.R., and Tabin, C.J. (2004). Bmp4 and morphological variation of beaks in Darwin's finches. Science *305*, 1462–1465.

Adamska, M., Wolff, A., Kreusler, M., Wittbrodt, J., Braun, T., and Bober, E. (2001). Five Nkx5 genes show differential expression patterns in anlagen of sensory organs in medaka: insight into the evolution of the gene family. Dev. Genes Evol. *211*, 338–349.

Ai, X., Cappuzzello, J., and Hall, A.K. (1999). Activin and bone morphogenetic proteins induce calcitonin gene-related peptide in embryonic sensory neurons in vitro. Mol. Cell. Neurosci. *14*, 506–518.

Anderson, D.J. (1999). Lineages and transcription factors in the specification of vertebrate primary sensory neurons. Curr. Opin. Neurobiol. *9*, 517–524.

Arber, S., Ladle, D.R., Lin, J.H., Frank, E., and Jessell, T.M. (2000). ETS gene Er81 controls the formation of functional connections between group Ia sensory afferents and motor neurons. Cell *101*, 485–498.

Ayer-Le Lievre, C.S., and Le Douarin, N.M. (1982). The early development of cranial sensory ganglia and the potentialities of their component cells studied in quail-chick chimeras. Dev. Biol. *94*, 291–310.

Baker, C.V., Stark, M.R., Marcelle, C., and Bronner-Fraser, M. (1999). Competence, specification and induction of Pax-3 in the trigeminal placode. Development *126*, 147–156.

Baker, C.V., Stark, M.R., and Bronner-Fraser, M. (2002). Pax3-expressing trigeminal placode cells can localize to trunk neural crest sites but are committed to a cutaneous sensory neuron fate. Dev. Biol. *249*, 219–236.

Beaudreau, D.E., and Jerge, C.R. (1968). Somatotopic representation in the Gasserian ganglion of tactile peripheral fields in the cat. Arch. Oral Biol. *13*, 247–256.

Begbie, J., Ballivet, M., and Graham, A. (2002). Early steps in the production of sensory neurons by the neurogenic placodes. Mol. Cell. Neurosci. *21*, 502–511.

Biondi, C.A., Das, D., Howell, M., Islam, A., Bikoff, E.K., Hill, C.S., and Robertson, E.J. (2007). Mice develop normally in the absence of Smad4 nucleocytoplasmic shuttling. Biochem. J. *404*, 235–245.

Borsook, D., DaSilva, A.F., Ploghaus, A., and Becerra, L. (2003). Specific and somatotopic functional magnetic resonance imaging activation in the trigeminal ganglion by brush and noxious heat. J. Neurosci. *23*, 7897–7903.

Campenot, R.B. (1982). Development of sympathetic neurons in compartmentalized cultures. II. Local control of neurite survival by nerve growth factor. Dev. Biol. *93*, 13–21.

Chai, Y., Jiang, X., Ito, Y., Bringas, P., Jr., Han, J., Rowitch, D.H., Soriano, P., McMahon, A.P., and Sucov, H.M. (2000). Fate of the mammalian cranial neural crest during tooth and mandibular morphogenesis. Development *127*, 1671–1679.

Chen, A.I., de Nooij, J.C., and Jessell, T.M. (2006a). Graded activity of transcription factor Runx3 specifies the laminar termination pattern of sensory axons in the developing spinal cord. Neuron *49*, 395–408.

Chen, C.L., Broom, D.C., Liu, Y., de Nooij, J.C., Li, Z., Cen, C., Samad, O.A., Jessell, T.M., Woolf, C.J., and Ma, Q. (2006b). Runx1 determines nociceptive sensory neuron phenotype and is required for thermal and neuropathic pain. Neuron *49*, 365–377.

Chu, G.C., Dunn, N.R., Anderson, D.C., Oxburgh, L., and Robertson, E.J. (2004). Differential requirements for Smad4 in TGFbeta-dependent patterning of the early mouse embryo. Development *131*, 3501–3512.

Clotman, F., Lannoy, V.J., Reber, M., Cereghini, S., Cassiman, D., Jacquemin, P., Roskams, T., Rousseau, G.G., and Lemaigre, F.P. (2002). The onecut transcription factor HNF6 is required for normal development of the biliary tract. Development *129*, 1819–1828.

Clotman, F., Jacquemin, P., Plumb-Rudewiez, N., Pierreux, C.E., Van der Smissen, P., Dietz, H.C., Courtoy, P.J., Rousseau, G.G., and Lemaigre, F.P. (2005). Control of liver cell fate decision by a gradient of TGF beta signaling modulated by Onecut transcription factors. Genes Dev. *19*, 1849–1854.

Coll, M., Seidman, J.G., and Muller, C.W. (2002). Structure of the DNA-bound T-box domain of human TBX3, a transcription factor responsible for ulnar-mammary syndrome. Structure (Camb.) *10*, 343–356.

Dunn, N.R., Winnier, G.E., Hargett, L.K., Schrick, J.J., Fogo, A.B., and Hogan, B.L. (1997). Haploinsufficient phenotypes in Bmp4 heterozygous null mice and modification by mutations in Gli3 and Alx4. Dev. Biol. *188*, 235–247.

Erzurumlu, R.S., and Jhaveri, S. (1992). Trigeminal ganglion cell processes are spatially ordered prior to the differentiation of the vibrissa pad. J. Neurosci. *12*, 3946–3955.

Frank, E., and Wenner, P. (1993). Environmental specification of neuronal connectivity. Neuron *10*, 779–785.

Fundin, B.T., Silos-Santiago, I., Ernfors, P., Fagan, A.M., Aldskogius, H., DeChiara, T.M., Phillips, H.S., Barbacid, M., Yancopoulos, G.D., and Rice, F.L. (1997). Differential dependency of cutaneous mechanoreceptors on neurotrophins, trk receptors, and P75 LNGFR. Dev. Biol. *190*, 94–116.

Furuta, Y., and Hogan, B.L. (1998). BMP4 is essential for lens induction in the mouse embryo. Genes Dev. *12*, 3764–3775.

Ginty, D.D., and Segal, R.A. (2002). Retrograde neurotrophin signaling: Trk-ing along the axon. Curr. Opin. Neurobiol. *12*, 268–274.

Glebova, N.O., and Ginty, D.D. (2005). Growth and survival signals controlling sympathetic nervous system development. Annu. Rev. Neurosci. *28*, 191–222.

Graef, I.A., Wang, F., Charron, F., Chen, L., Neilson, J., Tessier-Lavigne, M., and Crabtree, G.R. (2003). Neurotrophins and netrins require calcineurin/NFAT signaling to stimulate outgrowth of embryonic axons. Cell *113*, 657–670.

Guha, U., Gomes, W.A., Samanta, J., Gupta, M., Rice, F.L., and Kessler, J.A. (2004). Target-derived BMP signaling limits sensory neuron number and the extent of peripheral innervation in vivo. Development *131*, 1175–1186.

Hall, A.K., Dinsio, K.J., and Cappuzzello, J. (2001). Skin cell induction of calcitonin gene-related peptide in embryonic sensory neurons in vitro involves activin. Dev. Biol. *229*, 263–270.

Hippenmeyer, S., Kramer, I., and Arber, S. (2004). Control of neuronal phenotype: what targets tell the cell bodies. Trends Neurosci. *27*, 482–488.

Howe, C.L., and Mobley, W.C. (2005). Long-distance retrograde neurotrophic signaling. Curr. Opin. Neurobiol. *15*, 40–48.

Huang, E.J., Wilkinson, G.A., Farinas, I., Backus, C., Zang, K., Wong, S.L., and Reichardt, L.F. (1999a). Expression of Trk receptors in the developing mouse trigeminal ganglion: in vivo evidence for NT-3 activation of TrkA and TrkB in addition to TrkC. Development *126*, 2191–2203.

Huang, E.J., Zang, K., Schmidt, A., Saulys, A., Xiang, M., and Reichardt, L.F. (1999b). POU domain factor Brn-3a controls the differentiation and survival of trigeminal neurons by regulating Trk receptor expression. Development *126*, 2869–2882.

Inoue, K., Ozaki, S., Shiga, T., Ito, K., Masuda, T., Okado, N., Iseda, T., Kawaguchi, S., Ogawa, M., Bae, S.C., et al. (2002). Runx3 controls the axonal projection of proprioceptive dorsal root ganglion neurons. Nat. Neurosci. *5*, 946–954.

Jacquemin, P., Lannoy, V.J., Rousseau, G.G., and Lemaigre, F.P. (1999). OC-2, a novel mammalian member of the ONECUT class of homeodomain transcription factors whose function in liver partially overlaps with that of hepatocyte nuclear factor-6. J. Biol. Chem. *274*, 2665–2671.

Jacquemin, P., Lemaigre, F.P., and Rousseau, G.G. (2003a). The One-cut transcription factor HNF-6 (OC-1) is required for timely specification of the pancreas and acts upstream of Pdx-1 in the specification cascade. Dev. Biol. *258*, 105–116.

Jacquemin, P., Pierreux, C.E., Fierens, S., van Eyll, J.M., Lemaigre, F.P., and Rousseau, G.G. (2003b). Cloning and embryonic expression pattern of the mouse Onecut transcription factor OC-2. Gene Expr. Patterns *3*, 639–644.

Jiang, X., Rowitch, D.H., Soriano, P., McMahon, A.P., and Sucov, H.M. (2000). Fate of the mammalian cardiac neural crest. Development *127*, 1607–1616.

Keshishian, H., and Kim, Y.S. (2004). Orchestrating development and function: retrograde BMP signaling in the Drosophila nervous system. Trends Neurosci. *27*, 143–147.

Killackey, H.P., Rhoades, R.W., and Bennett-Clarke, C.A. (1995). The formation of a cortical somatotopic map. Trends Neurosci. *18*, 402–407.

Knecht, A.K., and Bronner-Fraser, M. (2002). Induction of the neural crest: a multigene process. Nat. Rev. Genet. *3*, 453–461.

Kramer, I., Sigrist, M., de Nooij, J.C., Taniuchi, I., Jessell, T.M., and Arber, S. (2006). A role for Runx transcription factor signaling in dorsal root ganglion sensory neuron diversification. Neuron *49*, 379–393.

Lawson, K.A., Dunn, N.R., Roelen, B.A., Zeinstra, L.M., Davis, A.M., Wright, C.V., Korving, J.P., and Hogan, B.L. (1999). Bmp4 is required for the generation of primordial germ cells in the mouse embryo. Genes Dev. *13*, 424–436.

Levy, L., and Hill, C.S. (2005). Smad4 dependency defines two classes of transforming growth factor {beta} (TGF-{beta}) target genes and distinguishes TGF-{beta}-induced epithelial-mesenchymal transition from its antiproliferative and migratory responses. Mol. Cell. Biol. *25*, 8108–8125.

Li, Y., Erzurumlu, R.S., Chen, C., Jhaveri, S., and Tonegawa, S. (1994). Whisker-related neuronal patterns fail to develop in the trigeminal brainstem nuclei of NMDAR1 knockout mice. Cell *76*, 427–437.

Li, W., Qiao, W., Chen, L., Xu, X., Yang, X., Li, D., Li, C., Brodie, S.G., Meguid, M.M., Hennighausen, L., and Deng, C.X. (2003). Squamous cell carcinoma and mammary abscess formation through squamous metaplasia in Smad4/Dpc4 conditional knockout mice. Development *130*, 6143–6153.

Liu, W., Selever, J., Wang, D., Lu, M.F., Moses, K.A., Schwartz, R.J., and Martin, J.F. (2004). Bmp4 signaling is required for outflow-tract septation and branchial-arch artery remodeling. Proc. Natl. Acad. Sci. USA *101*, 4489–4494.

Marmigere, F., Montelius, A., Wegner, M., Groner, Y., Reichardt, L.F., and Ernfors, P. (2006). The Runx1/AML1 transcription factor selectively regulates development and survival of TrkA nociceptive sensory neurons. Nat. Neurosci. *9*, 180–187.

Massague, J., and Gomis, R.R. (2006). The logic of TGFbeta signaling. FEBS Lett. *580*, 2811–2820.

Nohe, A., Keating, E., Knaus, P., and Petersen, N.O. (2004). Signal transduction of bone morphogenetic protein receptors. Cell. Signal. *16*, 291–299.

O'Connor, R., and Tessier-Lavigne, M. (1999). Identification of maxillary factor, a maxillary process-derived chemoattractant for developing trigeminal sensory axons. Neuron *24*, 165–178.

Patel, T.D., Jackman, A., Rice, F.L., Kucera, J., and Snider, W.D. (2000). Development of sensory neurons in the absence of NGF/TrkA signaling in vivo. Neuron *25*, 345–357.

Patel, T.D., Kramer, I., Kucera, J., Niederkofler, V., Jessell, T.M., Arber, S., and Snider, W.D. (2003). Peripheral NT3 signaling is required for ETS protein expression and central patterning of proprioceptive sensory afferents. Neuron *38*, 403–416.

Ritter, A.M., and Frank, E. (1999). Peripheral specification of Ia synaptic input to motoneurons innervating foreign target muscles. J. Neurobiol. *41*, 471–481.

Scott, L., and Atkinson, M.E. (1999). Compartmentalisation of the developing trigeminal ganglion into maxillary and mandibular divisions does not depend on target contact. J. Anat. *195*, 137–145.

Stottmann, R.W., Choi, M., Mishina, Y., Meyers, E.N., and Klingensmith, J. (2004). BMP receptor IA is required in mammalian neural crest cells for development of the cardiac outflow tract and ventricular myocardium. Development *131*, 2205–2218.

Waite, P.M.E., and Tracey, D.J. (1995). Trigeminal sensory system. In The Rat Nervous System, G. Paxinos, ed. (San Diego, CA: Academic Press), pp. 705–724.

Wang, G., and Scott, S.A. (1997). Muscle sensory innervation patterns in embryonic chick hindlimbs following dorsal root ganglion reversal. Dev. Biol. *186*, 27–35.

Wang, G., and Scott, S.A. (1999). Independent development of sensory and motor innervation patterns in embryonic chick hindlimbs. Dev. Biol. *208*, 324–336.

Wenner, P., and Frank, E. (1995). Peripheral target specification of synaptic connectivity of muscle spindle sensory neurons with spinal motoneurons. J. Neurosci. *15*, 8191–8198.

Wu, P., Jiang, T.X., Suksaweang, S., Widelitz, R.B., and Chuong, C.M. (2004). Molecular shaping of the beak. Science *305*, 1465–1466.

Xu, P., Van Slambrouck, C., Berti-Mattera, L., and Hall, A.K. (2005). Activin induces tactile allodynia and increases calcitonin gene-related peptide after peripheral inflammation. J. Neurosci. *25*, 9227–9235.

Yang, X., Li, C., Herrera, P.L., and Deng, C.X. (2002). Generation of Smad4/Dpc4 conditional knockout mice. Genesis *32*, 80–81.

Yang, L., Cai, C.L., Lin, L., Qyang, Y., Chung, C., Monteiro, R.M., Mummery, C.L., Fishman, G.I., Cogen, A., and Evans, S. (2006). Isl1Cre reveals a common Bmp pathway in heart and limb development. Development *133*, 1575–1585.

Yoshikawa, M., Senzaki, K., Yokomizo, T., Takahashi, S., Ozaki, S., and Shiga, T. (2007). Runx1 selectively regulates cell fate specification and axonal projections of dorsal root ganglion neurons. Dev. Biol. *303*, 663–674.